Trapping effects and acoustoelectric current saturation in ZnO single crystals

Mosekilde, Erik

Published in:
Physical Review B Condensed Matter

Link to article, DOI:
10.1103/PhysRevB.2.3234

Publication date:
1970

Document Version
Publisher's PDF, also known as Version of record

ping phenomena induced by the magnetic field, e.g., magnetoresistivity in the hopping region.[1-4,10-12,15-17]

ACKNOWLEDGMENTS

The author wishes to express his gratitude to Dr. J. Mycielski and to Professor M. Suffczyński for many valuable discussions and remarks, and to J. Trylski for communication of his results before publication.

[1]P. Csavinszky, Phys. Rev. 119, 1605 (1960).
[2]N. Mikoshiba and S. J. Gonda, Phys. Rev. 127, 1954 (1962).
[3]N. Mikoshiba, Phys. Rev. 127, 1962 (1962).
[4]N. Mikoshiba, J. Phys. Chem. Solids 24, 341 (1963).
[5]J. Blinowski and J. Mycielski, Phys. Rev. 136, A266 (1964); 140, A1024 (1965).
[6]J. Blinowski, Phys. Rev. 147, 547 (1966).
[7]N. Van Huong, Acta Phys. Polon. 33, 635 (1968).
[8]J. Trylski (unpublished).
[9]T. Holstein, Phys. Rev. 124, 1329 (1961).
[10]H. Fritzche and K. Lark-Horovitz, Physica 20, 834 (1954).
[11]R. J. Sladek and R. W. Keyes, Phys. Rev. 122, 437 (1961).
[12]C. Yamanouchi and W. Sasaki, J. Phys. Soc. Japan 17, 1664 (1962).
[13]R. C. Milward and L. J. Neuringer, Phys. Rev. Letters 15, 664 (1965).
[14]R. C. Milward and L. Aggarwal, J. Phys. Soc. Japan Suppl. 21, 582 (1966).
[15]J. A. Chroboczek and R. J. Sladek, Phys. Rev. 151, 595 (1966).
[16]W. W. Lee and R. J. Sladek, Phys. Rev. 158, 788 (1967).
[17]J. A. Chroboczek, E. W. Prohofsky, and R. J. Sladek, Phys. Letters 24A, 657 (1967); Phys. Rev. 169, 593 (1968).
[18]A. Miller and E. Abrahams, Phys. Rev. 120, 745 (1960).
[19]H. Gummel and M. Lax, Ann. Phys. (N.Y.) 2, 28 (1957).
[20]A. Myszkowski and M. Rogala, Phys. Rev. 168, 768 (1968).
[21]A. Myszkowski, J. Phys. Chem. Solids (to be published).
[22]J. Mycielski, Phys. Rev. 125, 46 (1962).
[23]E. O. Kane, Phys. Rev. 119, 40 (1960).
[24]K. Takeyama, J. Phys. Soc. Japan 23, 1013 (1967).

PHYSICAL REVIEW B VOLUME 2, NUMBER 8 15 OCTOBER 1970

Trapping Effects and Acoustoelectric Current Saturation in ZnO Single Crystals

E. Mosekilde
Physics Department III, The Technical University of Denmark, Lyngby, Denmark
(Received 2 June 1970)

Measurements of current-voltage characteristics for ZnO single crystals at temperatures between 77 and 640 °K are reported. Because of the buildup of an intense acoustic flux, a strong current saturation sets in when the trap-controlled electron drift velocity is equal to the velocity of sound. The temperature dependence of the saturated current is discussed in terms of a trapping model which includes nonlinear trapping effects. Our results indicate the presence of a shallow-donor level with an ionization energy of 50 meV and a deep-donor level approximately 230 meV below the conduction-band edge. The capture cross section for the shallow donors is determined to be about 5×10^{-12} cm^2 at 100 °K.

I. INTRODUCTION

The electronic properties of ZnO single crystals have been studied by Hutson,[1] who measured the Hall coefficient and the electrical conductivity at temperatures between 55 and 300 °K. By analyzing the temperature dependence of the free-electron density, Hutson obtained a donor ionization energy of 51 meV for hydrogen, zinc, and lithium donors.

Alternatively to Hall experiments, the electronic properties of piezoelectric semiconductors can be studied by means of the acoustoelectric current saturation.[2,3] This method was first employed by Moore and Smith[4] to investigate single crystals of semiconducting CdS. Subsequently, Rannestad[5] has determined the density and ionization energy of impurity states in photoconducting CdS by measuring the temperature dependence of the threshold field for current saturation. For ZnO, a preliminary discussion of the temperature dependence of the saturated current density was given by Meyer *et al.*[6] Below 200 °K, the experimental results could be explained in terms of the ionization of shallow donors with an activation energy between 40 and 70 meV. To account for the increase in saturated current at temperatures above 200 °K, the additional presence of a deep-donor level had to be assumed.

The acoustoelectric current saturation is associated with the internal generation of a high-intensity acoustic flux which is built up from the thermal background of long-wavelength lattice vibrations by virtue of the acoustoelectric interaction.[7,8] In a semiconductor which contains fully ionized impurity states only, the drifting carriers will start to feed energy into the sound flux when their drift velocity is equal to the velocity of sound. The steady reaction of the growing sound waves on the carriers can be expressed in terms of an acoustoelectric current which opposes the drift current.[9] Weinreich[10] gives an expression for the acoustoelectric current in terms of the rate of change of the acoustic energy density.

In an n-type semiconductor which contains a partially ionized donor level in communication with the conduction band, the acoustically produced space charge may divide into waves of free and bound charge. Electron trapping is then said to take place. Effects of carrier trapping were considered by Hutson and White[7] in their original paper on acoustoelectric coupling. They assumed the bound charge to equilibrate with the free charge of the conduction band in times short compared to an acoustic period. In this case, the two space-charge waves will be in phase with a fraction f_0 (the trapping factor) of the total space charge being mobile. Carrier trapping was shown to shift the threshold drift velocity for acoustic amplification from the velocity of sound v_s to v_s/f_0. This treatment has subsequently been extended by Uchida *et al.*[11] to take into account effects of frequency-dependent trapping. Because of the phase difference which develops between mobile and trapped space-charge waves when the relaxation time for carrier trapping is comparable to the acoustic period, an additional shift of the threshold drift velocity for acoustic gain arises.

To realize current saturation, besides acoustic amplification we also need an opposing acoustoelectric current. Greebe[12,13] and Southgate and Spector[14] have generalized the Weinreich relation to take into account linear trapping effects. As pointed out by Katilyus,[15] however, a consistent calculation of the acoustoelectric current must treat carrier trapping to second order in the wave amplitudes. Nonlinear trapping contributes to the acoustoelectric current an additional term which arises from the ionization of donor states by the acoustic flux. Katilyus confined himself to a discussion of the case of a rapid trap relaxation. In the present paper, we extend his treatment to take finite equilibration rates into account.

Theoretical considerations show that in the case of frequency-independent trapping, the threshold drift velocity for acoustoelectric current saturation in ZnO will be determined by nonlinear trapping rather than by linear trapping. For our ZnO crystals, frequency-independent trapping is supposed to take place at temperatures between 100 and 150 °K.[6] We have analyzed the variation of the saturated current in this temperature range in terms of both linear and nonlinear trapping effects. Assuming linear trapping to determine the threshold drift velocity, we obtain for the shallow-donor level an ionization energy of 40 meV. Including, however, in our analyses nonlinear trapping effects, the same energy was determined as $E_{D1} = 50$ meV, which is in close accordance with the value stated by Hutson.[1] Thus we conclude that nonlinear trapping can be important in determining the threshold for current saturation.

At temperatures below 100 °K, the equilibration rate between free and bound states becomes insufficient for maintaining a local equilibrium distribution between mobile and trapped space charge. By analysing the temperature variation of the saturated current density in this region, we have determined the capture cross section for the shallow donors to be 5×10^{-12} cm^2 at 100 °K. Finally, the experimental results obtained at temperatures above 200 °K yield the ionization energy of the deep-donor states as $E_{D2} = 230$ meV.

II. BASIC THEORY

A. Linear Trapping

Consider an n-type semiconductor which contains a single type of shallow donor (density N_D and energy ϵ_D) partly compensated by deep acceptors (density $N_A < N_D$). Assume for simplicity a nondegenerate free-electron gas. The thermal equilibrium density of free electrons may then be expressed by

$$n_c = N_c\, e^{(\epsilon_F - \epsilon_c)/kT} . \tag{1}$$

Here $N_c = 2(2\pi m_c kT/h^2)^{3/2}$ is the effective density of states for the conduction band, m_c being the density-of-states mass and h Planck's constant. ϵ_c is the energy of the conduction-band edge, ϵ_F the Fermi energy, and kT the thermal energy. At the same time, the density of electrons remaining in the donor states is

$$n_D = N_D/(1 + g^{-1}\, e^{(\epsilon_D - \epsilon_F)/kT}) , \tag{2}$$

g being the statistical degeneracy factor for these states. The Fermi energy may be eliminated from Eqs. (1) and (2) to give

$$n_c(N_D - n_D)/N_c n_D = g^{-1}\, e^{-E_D/kT} , \tag{3}$$

with the donor activation energy $E_D = \epsilon_c - \epsilon_D$.

By generating a space-charge wave, an acoustic wave traveling through a piezoelectric semiconductor disturbs the equilibrium distribution of electrons

between free and bound states. Since the electron population of the conduction band continuously communicates with the population of bound electron states, a modulation of the free-electron density tends to induce a wave periodic variation of the density of bound electrons. Assuming the acceptor level to be completely occupied in thermal equilibrium, however, the density of electrons bound in acceptor states must remain unaffected by the sound wave.

Describing the equilibration rate between conduction band and donor states by the trap relaxation time τ, essentially no redistribution between free and bound states takes place as long as τ is long compared to the acoustic period. In the opposite limit of a short relaxation time, the electron redistribution will be practically immediate. In this case, a local instantaneous equilibrium is established in which free and bound space-charge waves travel in phase with a fraction f_0, the trapping factor, of the total space charge being mobile. In general, the communication may be insufficient to maintain a local equilibrium but still sufficient to cause the bound electron density to vary. A phase difference then develops between mobile and trapped space-charge waves which leads to a complex trapping factor.[11]

The average time τ_c that an electron spends in the conduction band before being captured into a bound state is

$$\tau_c^{-1} = v_{\text{th}} S_n (N_D - n_D) , \tag{4}$$

where v_{th} is the thermal electron velocity, S_n is the capture cross section, and $(N_D - n_D)$ the density of empty donors. In thermal equilibrium, the capture of electrons by traps must be balanced by the reverse process of reemission of electrons into the conduction band. Hence, the time τ_D required to escape from a trap is

$$\tau_D^{-1} = v_{\text{th}} S_n (N_D - n_D) n_c / n_D . \tag{5}$$

In the presence of an acoustic wave, the rate of change for the density of trapped electrons may be expressed by

$$\frac{\partial n^D}{\partial t} = v_{\text{th}} S_n (N_D - n^D) n^c - \frac{n^D}{\tau_D} , \tag{6}$$

where now n^c and n^D denote local instantaneous densities of free and trapped electrons, respectively. The first term on the right-hand side gives the rate at which free electrons are captured, whereas the second term gives the rate of reemission. τ_D is assumed to remain unchanged from its thermal equilibrium value as given by Eq. (5).

The complex trapping factor f may now be introduced by means of the equations

$$n^c = n_c + f n_s \tag{7}$$

and

$$n^D = n_D + (1 - f) n_s , \tag{8}$$

where n_s is the total electron density modulation for which we assume a sinusoidal solution

$$n_s = n_{s0} e^{i\omega (x/v_s - t)} . \tag{9}$$

Here ω is the angular acoustic frequency. As hitherto, n_c and n_D denote thermal equilibrium electron densities. By inserting (7) and (8) into (6), neglecting terms of second order in n_s, and solving for the real and the imaginary parts of the equation separately, we obtain for the trapping factor[11]

$$f = (f_0 - i\omega\tau)/(1 - i\omega\tau) , \tag{10}$$

with[7]

$$f_0^{-1} = 1 + n_D (N_D - n_D)/n_c N_D \tag{11}$$

and

$$\tau^{-1} = \tau_c^{-1} + \tau_D^{-1} + v_{\text{th}} S_n n_c , \tag{12}$$

where f gives the small signal ratio[16] between the free-electron density wave and the total electron-density wave n_s. The trapping factor clearly reduces to f_0 when $\omega\tau \ll 1$. In the opposite limit of a long trap relaxation time, f approaches unity and trapping effects disappear. Previously, Moore and Smith[4] obtained an expression for the trap relaxation time in which the term $v_{\text{th}} S_n n_c$ is lacking. This term arises when one allows for the fact that the time an electron spends in the conduction band has a wave periodic variation following the modulation of the empty donor density.

The influence of frequency-dependent trapping on acoustoelectric coupling has been discussed in detail by Uchida *et al.*[11] According to their analysis, frequency-dependent trapping shifts the threshold drift velocity for acoustic amplification to

$$v_{c1} = (v_s/bf_0)[1 + a(a + \omega/\omega_D)] , \tag{13}$$

where

$$\omega_D = v_s^2/bf_0 D_n \tag{14}$$

is the effective diffusion frequency, D_n being the electron diffusion constant. The real functions a and bf_0 are defined by

$$f = bf_0/(1 + ia) , \tag{15}$$

which can be solved to give

$$a = (1 - f_0)\omega\tau/(f_0 + \omega^2\tau^2) \tag{16}$$

and

$$bf_0 = (f_0^2 + \omega^2\tau^2)/(f_0 + \omega^2\tau^2) . \tag{17}$$

$\tan^{-1} a$ is the phase shift of the free-charge relative

to the total space-charge wave. Considered as a function of $\omega\tau$, a takes a maximum value of

$$a_m = (1 - f_0)/2f_0^{1/2} \tag{18}$$

for $\omega\tau = f_0^{1/2}$. Since a_m increases with decreasing f_0, we expect the phase-shift correction factor

$$d = 1 + a(a + \omega/\omega_D) \tag{19}$$

to be particularly important when f_0 is small.

B. Acoustoelectric Current Including Nonlinear Trapping

In Sec. II A, we considered manifestations of carrier trapping in the linear theory of acoustoelectric coupling. Doing so, we neglected the steady reaction of the sound wave upon the drifting carriers, the dc reaction being of second order in the wave amplitudes. As was first predicted by Parmenter, [17] the acoustic wave exerts an average drag on the carriers and, under short-circuit conditions, hereby produces a dc current. This is the acoustoelectric current. Using a general argument based on conservation of energy and momentum in the wave-carrier interaction, Weinreich[10] obtained a relation between the acoustoelectric current density j_{ae} and the rate of change of the acoustic energy density w,

$$j_{ae} = \mu \alpha_e w , \tag{20}$$

where μ is the carrier drift mobility and α_e the electronic part of the acoustic energy attenuation constant. If the carrier drift velocity exceeds the threshold for acoustic amplification, α_e will be negative, and the acoustoelectric current will oppose the drift current. As pointed out by Hutson, [9] the current saturation observed in piezoelectric semiconductors is caused by the opposing acoustoelectric current associated with the buildup of an intense acoustic flux from the thermal background noise. The thermal acoustic flux by itself is too weak to cause any appreciable acoustoelectric current and will have to be amplified by at least three orders of magnitude before deviations from Ohm's law can be observed. [18] Thus net acoustic gain as well as an opposing acoustoelectric current are required for acoustoelectric current saturation.

In its simple form [Eq. (20)], the Weinreich relation assumes the acoustic wave to interact with free carriers only and therefore has to be modified when carrier trapping occurs. Greebe[12,13] and Southgate and Spector [14] have generalized the Weinreich relation to take linear trapping into account.

By interacting with the sound wave, the free carriers gain forward momentum at a rate (per unit volume) [14]

$$j_{ae}/\mu = \tfrac{1}{2} q \,\mathrm{Re}(f n_s F_1^*) . \tag{21}$$

Here F_1 is the electric field generated by the acoustic wave and q is the carrier charge. Using the relations of Ref. 8 appropriately modified to take frequency-dependent trapping into account, $n_s F_1^*$ can be expressed in terms of the acoustic energy density to give

$$j_{ae} = -\mu w \gamma , \tag{22}$$

with

$$\gamma = \frac{K^2 \omega_C}{v_s} \frac{b f_0 y}{(y + a\omega_C/\omega)^2 + (a + \omega_C/\omega + \omega/\omega_D)^2} . \tag{23}$$

Here ω_C is the conductivity frequency in White's notation, [8] K is the electromechanical coupling constant, [8] and

$$y = (b f_0 v_d - v_s)/v_s \tag{24}$$

is the effective drift parameter, v_d being the carrier drift velocity. Note that the acoustoelectric current changes its sign at a drift velocity v_s/bf_0, whereas the threshold drift velocity for acoustic gain is v_{c1} as given by (13), so that, in general, the two thresholds need not coincide. [14] As pointed out by Katilyus [15] and also by Gulyaev, [19] the above discussion is incomplete because it treats carrier trapping in a linear approximation. Since the acoustoelectric current is a second-order effect, a consistent calculation of j_{ae} must consider carrier trapping to the second order in the wave amplitudes. [20] So far, the division of the total acoustically produced space charge into mobile and bound charge has been accounted for by introducing the trapping factor f. Considering effects of second order in the wave amplitudes, however, the number of excess electrons which are mobile no longer constitutes a space- and time-independent fraction of the total number of excess electrons. In particular, this means that whereas the total space charge in the weak coupling approximation averages to zero within an acoustic wavelength, the average number of excess conduction electrons may be finite. In the presence of a drift field, the change in the average density of free electrons contributes an additional term to the acoustoelectric current.

In his analysis, Katilyus considered a single type of trapping center only and assumed the trap relaxation time to be short. The theory of nonlinear trapping, however, is readily extended to permit arbitrary values for $\omega\tau$, as shown in the following.

At any given time, the rate of change of the density of trapped electrons is given by Eq. (6). Inserting now

$$n^c = n_c + f n_s + \delta n_c \tag{25}$$

and

$$n^D = n_D + (1 - f) n_s - \delta n_c , \tag{26}$$

where δn_c is the average change of the free-electron

density produced by nonlinear trapping, we obtain

$$\delta n_c = \tfrac{1}{2}(n_s n_s^*/n_c)\eta f_0 \,\mathrm{Re}\{f^*(1-f)\}, \tag{27}$$

where $\eta = n_D/N_D$ is the thermal equilibrium donor occupancy. A first-order approximation for δn_c is appropriate as long as $\delta n_c \ll n_c/\eta f_0$. Finally, $n_s n_s^*$ may be expressed in terms of the acoustic energy density to give

$$\delta n_c = \frac{K^2\omega_C}{v_s}\,\frac{(\mu w/qv_s)\eta f_0 b f_0(1-bf_0)}{(y+a\omega_C/\omega)^2+(a+\omega_C/\omega+\omega/\omega_D)^2}\,. \tag{28}$$

Note that δn_c will be positive or zero. An acoustic wave thus tends to increase the average density of free electrons. In the presence of a drift field F_0, the term δn_c gives an additional contribution to the acoustoelectric current so that

$$j_{ae} = \delta n_c q\mu F_0 - \mu\gamma w. \tag{29}$$

An important feature of the term $\delta n_c q\mu F_0$ is that it remains finite when, at a carrier drift velocity v_s/bf_0, the steady reaction of the sound wave on the carriers vanishes. Consequently, the change of sign for j_{ae} is displaced towards higher drift velocities. Using the relations (23) and (28) for γ and δn_c, the carrier drift velocity required to produce an opposing acoustoelectric current may be calculated to be

$$v_{c2} = v_s/[bf_0 - \eta f_0(1-bf_0)]. \tag{30}$$

We should like to stress that in deriving Eq. (30), we have considered a single-frequency acoustic wave only. The acoustoelectric current saturation, however, is due to the amplification of a vast number of thermal acoustic modes. Using (30) to predict the threshold drift velocity for an opposing acoustoelectric current in this case is then based upon the practical assumptions that (i) despite the spread in frequency and direction of propagation for the amplified waves, the dominant modes have coincident threshold drift velocities, and (ii) the threshold for any particular mode remains unaffected by the presence of other modes.

III. EXPERIMENTAL RESULTS

The ZnO crystals examined in the present work were provided by Nielsen. They were grown in this laboratory by the vapor-phase reaction method[21] with no intentional doping. Among the available crystals, we have selected some relatively small ones which appeared as colorless needles of regular hexagonal form and constant cross section. Usual crystal lengths and cross-sectional areas were about 4 mm and 0.4 mm^2, with the needle axis parallel to the sixfold c axis. Fired silver-paste contacts were found to be satisfactory for the present investigations.

To check the sample homogeneity at room temperature, a drift field of about 10 V/cm was applied to the crystal. The field distribution along the crystal surface was then measured by means of a resistive double probe having an interprobe distance of about 0.4 mm. Variations in the probe voltage of about 5%/mm sample length were found to be representative for most of our carefully selected crystals.

To measure the stationary current-voltage characteristic, square voltage pulses were applied to the crystal. The pulse length and repetition rate were usually 2 μsec and 10 pps, respectively, and the maximum attainable voltage was about 12 kV. The voltage drop across a 2-Ω series resistor was taken as a measure of the sample current, and appropriately attenuated current and voltage pulse signals were supplied to a dual channel sampling oscilloscope which provided dc output signals proportional to the pulse amplitudes at the sampling point. The sample temperature was varied between 77 and 640 °K. In the liquid-nitrogen to room-temperature range, the sample was cooled by means of nitrogen vapor, and the temperature was varied by heating the nitrogen gas. Experiments above room temperature were carried out with the sample mounted in a simple oven. At about 640 °K, sparking along the sample surface arose at the voltages needed for current saturation.

Figure 1 shows current-voltage characteristics

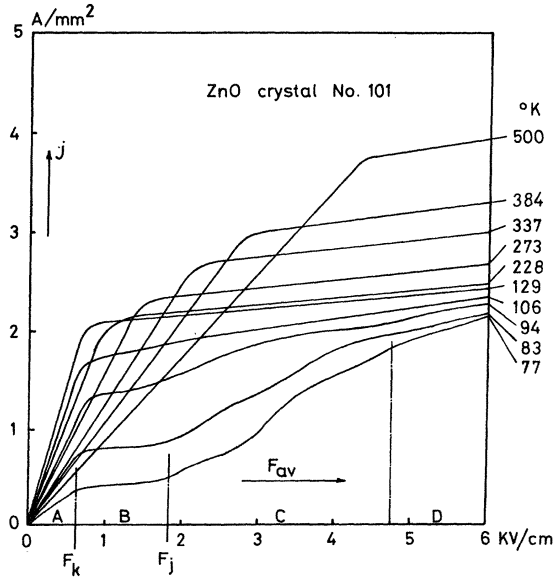

FIG. 1. Current density as a function of average applied field for ZnO crystal No. 101 at temperatures between 77 and 500 °K. The direction of current flow is parallel to the hexagonal axis.

for ZnO crystal No. 101 at various temperatures ranging from 77 to 500 °K. As the direction of current flow is parallel to the hexagonal axis, the current saturation is ascribed to amplification of off-axis shear waves[22] originating in the thermal acoustic flux. Rather similar characteristics were obtained for more than ten different samples.

At liquid-nitrogen temperature, the I-V curve exhibits four distinct regions: an almost Ohmic region A up to the knee field F_k where the curve breaks over into the first saturation region B. At F_j, the current jumps into a region C where different modes of current oscillations are found. Finally, at high average fields, a second current-saturation region D is reached. As the temperature is increased, the current in region B grows rather quickly until at about 110 °K it equals the saturation current of region D. At this temperature, the oscillation region disappears, and for higher temperatures only one saturation region is observed. From 129 to 228 °K, the saturation current is almost temperature independent, but above 228 °K, the saturation current again increases with temperature. As demonstrated by Meyer *et al.*,[6] this behavior of the current can be qualitatively explained in terms of a linear trapping model when assuming the presence of two kinds of trapping center. For one of these, the activation energy was found to be between 40 and 70 meV. Here we shall establish a quantitative description taking also nonlinear trapping into account. The trapping centers will be identified as shallow donors with an approximate activation energy of 50 meV and deep donors some 230 meV below the conduction-band edge.

From the knee-point field F_k and the corresponding current density j_k we may define an apparent electron mobility

$$\mu_k = v_s/F_k \tag{31}$$

and an apparent electron density

$$n_k = j_k/qv_s\,, \tag{32}$$

where $v_s = 2.7\times10^5$ cm/sec is the acoustic shear-wave velocity and q is to be understood as the elementary charge. n_k defines the number of electrons which, drifting at the velocity of sound, would cause the actually observed current at the knee point.

By defining the apparent electron mobility and the apparent electron density by Eqs. (31) and (32), we implicitly assume that the direction of propagation for the dominant acoustic waves is practically parallel to the direction of current flow. It is well known that the electromechanical coupling constant in ZnO vanishes for transverse acoustic waves traveling along the hexagonal axis[7] and that the current saturation in the case of electron flow parallel to the c axis must be ascribed to shear waves propagating at a small angle to the c axis.[6] When the off-axis propagation of the amplified sound waves is taken into account, the threshold drift velocity v_{c1} for acoustic gain as well as the threshold drift velocity v_{c2} for an opposing acoustoelectric current will be shifted upwards relative to the values given by (13) and (30). As long as the off-axis angle is smaller than 20°, however, the changes in the threshold drift velocities will be less than a few percent and, for the present discussion, the waves can be treated as propagating practically parallel to the c axis. In the case of current-saturated ZnO, the off-axis angle for the acoustic waves of maximum intensity has been determined by Brillouin scattering experiments[23] to be about 7°.

In Fig. 2, n_k has been plotted as a function of inverse temperature for four different samples. At 640 °K, practically all donors are ionized. As the temperature is decreased, more and more electrons are captured into deep-donor states until at about 210 °K, nearly all deep donors are occupied. At this temperature, the shallow donors start to capture electrons, and with further decreasing temperature, the density of free electrons will continue to decrease. However, because of trapping effects which permit bound electrons to participate in the acoustoelectric interaction, the apparent electron density remains almost independent of temperature. This continues until at about 110 °K, trapping effects are no longer able to maintain a constant apparent electron density. Below 110 °K, n_k decreases with decreasing temperature, partly because the trap relaxation time now becomes suf-

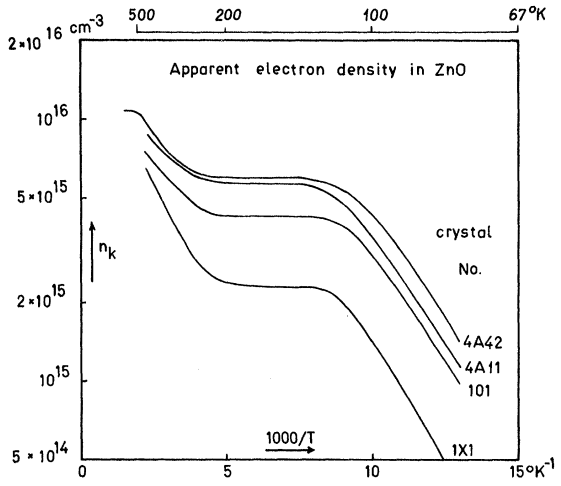

FIG. 2. Apparent electron density $n_k = j_k/qv_s$ as a function of temperature for four different ZnO crystals. j_k is the current density at the knee point of the I–V curves, q the elementary charge, and v_s the acoustic shear-wave velocity.

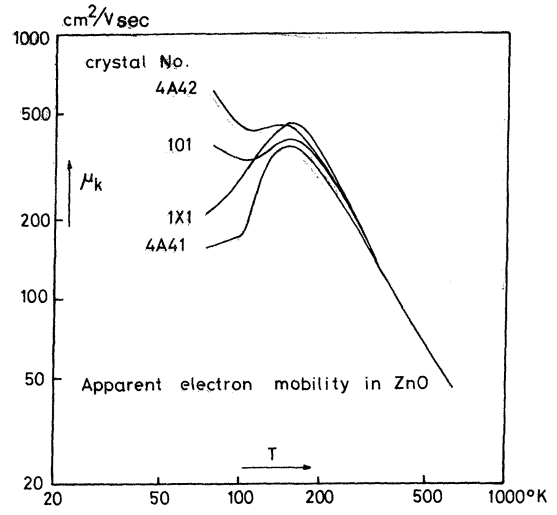

FIG. 3. Apparent electron mobility $\mu_k = v_s/F_k$ as a function of temperature for four different ZnO crystals. F_k is the knee point field of the I–V curves and v_s the acoustic shear-wave velocity.

ficiently long to reduce the communication between free and bound states.

From the above qualitative discussion, it appears justifiable to identify the plateau level for n_k at high temperatures (above 600 °K) with $N_{D2}+N_{D1}-N_A$, where N_{22} is the density of deep donors, N_{D1} the density of shallow donors, and N_A the density of compensating acceptors. $N_{D2}+N_{D1}-N_A$ is the maximum density of conduction electrons available at temperatures sufficiently low for intrinsic conductivity to be negligible. Correspondingly, we identify the plateau level for n_k at temperatures between 210 and 110 °K with $N_{D1}-N_A$. Thus, N_{D2} and $N_{D1}-N_A$ can be determined in a simple way from the curves of Fig. 1. For crystal No. 4A42, we obtain $N_{D2}=4.8\times10^{15}$ cm^{-3} and $N_{D1}-N_A=6.0\times10^{15}$ cm^{-3}. Hall measurements[24] on the same crystal indicate that $N_{D2}>2\times10^{15}$ cm^{-3} and $N_{D1}-N_A=3.9\times10^{15}$ cm^{-3}. In comparing these results, one will have to allow for the Hall factor which tends to reduce the carrier density obtained from Hall measurements relative to the true free-electron density. Also, neither our experiments nor the Hall measurements are particularly accurate in determining absolute values for the impurity densities.

Figure 3 shows the variation of μ_k with temperature for four different samples. From the form of the Hall mobility-versus-temperature curves,[1,24] it is concluded that different scattering mechanisms dominate the carrier momentum relaxation at different temperatures. The decrease of μ_k at temperatures above 150 °K can thus be ascribed to the onset of polar optical scattering. On the other hand, ionized impurity scattering is probably more important below 100 °K. In the transition region between these two scattering mechanisms, piezoelectric scattering may effectively limit the electron mobility. We shall not discuss the above curves in detail since our analysis of the electronic properties of ZnO is entirely based upon the variation of n_k. It should be noticed, however, that the rather sudden decrease of μ_k for temperatures below 150 °K is not observed in Hall mobility–versus–temperature curves.[24] This decrease of μ_k can be ascribed to trapping effects.

The Ohmic part of the I-V curves defines the sample resistance. The specific conductivity σ and the conductivity frequency $\omega_C=\sigma/\epsilon$ can then be calculated for known sample dimensions. Here $\epsilon=7.5\times10^{-11}$ F/m[1] is the static dielectric constant. The effective diffusion frequency

$$\omega_D = v_s^2/bf_0D_n = v_s^2 q/bf_0\mu k T \qquad (14')$$

is a little more difficult to obtain. For a first approach, however, we shall replace $bf_0\mu$ in Eq. (14) by μ_k, so that

$$\omega_D = qF_kv_s/kT. \qquad (33)$$

In Fig. 4, we have plotted ω_C and ω_D as functions of temperature for crystal No. 4A42. The frequency $\omega_M=(\omega_C\omega_D)^{1/2}$ has also been indicated. Notice how $\omega_M\approx8\times10^{10}$ sec^{-1} for this crystal turns out to be almost independent of temperature. At high temperatures where the trap relaxation time is

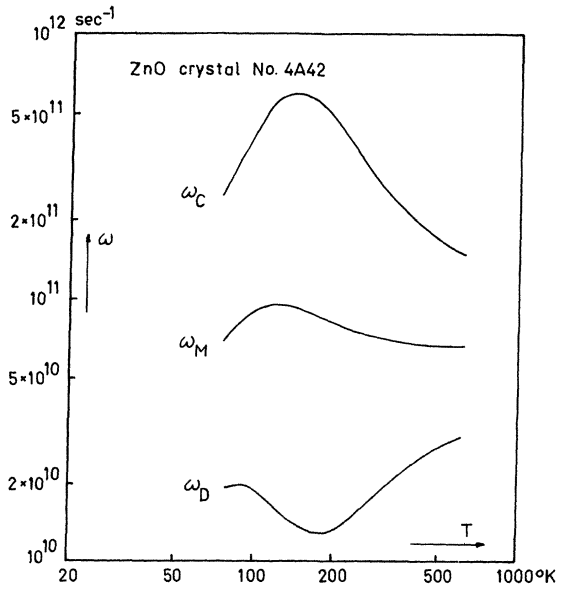

FIG. 4. Conductivity frequency ω_C, the diffusion frequency ω_D, and the frequency of maximum electronic gain $\omega_M=(\omega_C\omega_D)^{1/2}$ as functions of temperature for ZnO crystal No. 4A42. Note that ω_M is almost temperature independent.

short, ω_M is the frequency of maximum linear gain.[7,8] When, at temperatures below 100 °K, the trapping factor becomes complex (see below), no simple expression exists for the frequency of maximum gain. Nevertheless, we shall assume this latter frequency to be given by ω_M at all temperatures investigated and, moreover, we shall employ the simplification of taking $\omega_M = 8\times10^{10}\,\mathrm{sec}^{-1}$ independent of temperature.

So far, we have neglected nonelectronic losses. Because of the frequency dependence of the lattice losses, the dominant acoustic frequency generally falls below ω_M. If the lattice losses vary proportional to ω^p, net acoustic gain is first realized at a frequency[25]

$$\omega_m = [(2-p)/(2+p)]^{1/2}\omega_M \ . \tag{34}$$

Assuming $p = 1.62$,[26] we obtain $\omega_m = 2.6\times10^{10}\,\mathrm{sec}^{-1}$. As the drift field is increased beyond this first threshold, the frequency of maximum net gain increases and approaches ω_M in the limit where lattice losses can be neglected compared to electronic gain. At the threshold for current saturation, we expect the dominant acoustic frequency to fall somewhere between ω_m and ω_M. No serious reduction in accuracy will result from assuming the dominant acoustic frequency for crystal No. 4A42 to be equal to $\frac{1}{2}\omega_M$:

$$\omega = 4\times10^{10}\,\mathrm{sec}^{-1} \tag{35}$$

at all temperatures. At this frequency, the drift parameter required for electronic gain to overcome nonelectronic losses is

$$y = 25\alpha_L v_s/2K^2\omega_D = 1.04, \tag{36}$$

indicating that the threshold for net acoustic gain will be displaced about 4% relative to the threshold for electronic amplification. Here we have inserted $K^2 = 0.15$[27] and $\omega_D = 2\times10^{10}\,\mathrm{sec}^{-1}$. At room temperature, Hemphill[26] has measured the nonelectronic losses in ZnO for frequencies up to 1 GHz. We have extrapolated these results to obtain $\alpha_L = 300$ dB/cm at $\omega = 4\times10^{10}\,\mathrm{sec}^{-1}$.

IV. INTERPRETATION OF EXPERIMENTS

A. Experimental Evidence for Nonlinear Trapping

At temperatures above 250 °K, nearly all shallow donors are ionized. With decreasing temperature, the thermal equilibrium density of free electrons n_c decreases because more and more electrons are captured into shallow-donor states. At the same time, the possibility of wave periodic modulations in the occupancy of these bound states arises and consequently trapping effects can be expected. Note that because practically all deep donors will be occupied at temperatures below 250 °K, our problem is essentially a single-trap-level problem which can be discussed in terms of the trapping theory outlined in Sec. II.

Taking all deep donors as well as all acceptors to be occupied, the condition of neutrality reads

$$N_{D1} = N_A + n_c + n_{D1} \ , \tag{37}$$

where n_{D1} is the thermal equilibrium density of electrons bound in shallow-donor states. By means of (37), $n_D = n_{D1}$ can be eliminated from (3) and (11) to give

$$\frac{n_c(n_c+N_A)}{N_c(N_{D1}-N_A-n_c)} = g^{-1}\, e^{-E_{D1}/kT} \tag{38}$$

and

$$f_0^{-1} = 1 + (N_{D1}-N_A-n_c)(n_c+N_A)/n_c N_{D1} \ . \tag{39}$$

Likewise, n_{D1} may be eliminated from (4) and (5). Inserting τ_c and τ_D into (12), then, we obtain for the trap relaxation time

$$\tau^{-1} = v_{\mathrm{th}} S_n[(N_{D1}-N_A)(N_A+n_c)/(N_{D1}-N_A-n_c)+n_c]. \tag{40}$$

According to Eq. (40), τ will be small at relative high temperatures where the electron capture into shallow-donor states has just begun. At these temperatures, we assume the communication between free and bound states to be sufficiently rapid for the electrons to completely redistribute themselves within an acoustic period ($\omega\tau \ll 1$). In this case, $bf_0 = f_0$ and $a = 0$. Further, neglect of compensational effects ($N_A \ll n_c,\ N_{D1}$) leads to

$$f_0 = N_{D1}/(2N_{D1}-n_c) \tag{41}$$

and

$$\eta f_0 = f_0 n_{D1}/N_{D1} = 1 - f_0. \tag{42}$$

The threshold drift velocity v_{c1} for electronic gain and the threshold drift velocity v_{c2} for an opposing acoustoelectric current will then be given by

$$v_{c1} = v_s/f_0 \tag{43}$$

and

$$v_{c2} = v_s/[f_0 - (1-f_0)^2], \tag{44}$$

respectively.

As the occupancy of the shallow-donor states increases, according to (41), f_0 will gradually decrease from unity towards one-half. During most of this decrease,

$$v_{c2}/v_{c1} = f_0/[f_0-(1-f_0)^2] > 1.04, \tag{45}$$

so that v_{c2} will be greater than the threshold drift velocity for net acoustic gain. Under these circumstances, we expect the threshold for current saturation to be determined by nonlinear rather than by linear trapping. Note, however, that this situation

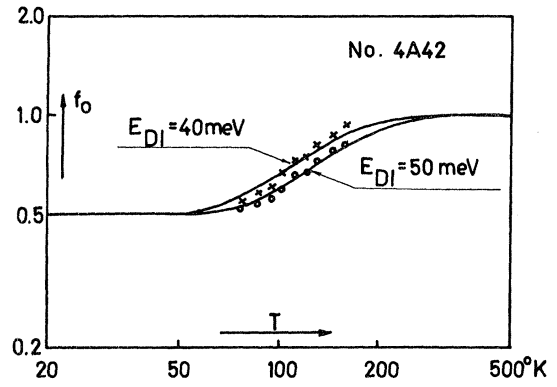

FIG. 5. Trapping factor f_0 as a function of temperature for crystal No. 4A42. The two theoretical curves were calculated for a shallow-donor ionization energy of 40 and 50 meV, respectively. The two sets of experimental points were obtained by analyzing the temperature variation of the apparent electron density n_k in terms of linear (crosses) and nonlinear (circles) trapping effects, respectively. Compensational effects as well as frequency-dependent trapping effects were neglected.

with dominant nonlinear trapping arises because of the large electronic gain factors that can be attained in ZnO. In other materials such as CdS and GaAs, a larger drift parameter is required for electronic gain to overcome nonelectronic losses, and, consequently, nonlinear trapping effects will be less prominent.

To compare the consequences of applying the linear or the nonlinear trapping theory to analyze our experimental results, we define the critical electron densities

$$n_{c1} = n_c v_{c1}/v_s = n_c/f_0 \tag{46}$$

and

$$n_{c2} = n_c v_{c2}/v_s = n_c/[f_0 - (1-f_0)^2]. \tag{47}$$

Assuming linear trapping effects to determine the threshold for current saturation, we may substitute $n_k = n_{c1}$.[28] n_c can then be eliminated from (41) and (46) to give a relation between f_0 and $n_k/N_{D1} = n_k(T)/n_k$ (200 °K) (for $T \leq 200$ °K). By means of this relation, we have plotted in Fig. 5 (crosses) f_0 as a function of temperature for crystal No. 4A42. On the other hand, assuming nonlinear trapping to determine the threshold for current saturation, we substitute $n_k = n_{c2}$. Eliminating now n_c from Eqs. (41) and (47), we find another relation between f_0 and $n_k(T)/n_k(200\ °K)$. This latter relation was used to obtain a new set of experimental points (circles in Fig. 5) for the variation of f_0 with temperature. Finally, we have plotted in this figure (solid curve) two theoretical curves for the variation of f_0 with temperature corresponding to $E_{D1} = 40$ and 50 meV, respectively. These curves were calculated from (41) with n_c as given by (38). We have used $N_{D1} = 6.0 \times 10^{15}$ cm^{-3} and $N_A = 0$ (consistent with our neglect of compensational effects). Further, we have taken for the effective density-of-states mass $m_c = 0.29\, m_0$[29] and for the donor degeneracy factor $g = 2$.[1]

From the distribution of the experimental points relative to the theoretical curves, we conclude that, applying the linear trapping theory to analyze our measurements, one would arrive at a donor activation energy of about 40 meV. Applying, on the other hand, the nonlinear trapping theory, the shallow-donor activation energy is determined to be about 50 meV. These results should be compared with an ionization energy of 51 meV obtained by Hutson[1] and particularly with an activation energy of 52 meV determined by Hall measurements on crystal No. 4A42.[24] The better agreement between our results and other independent results is thus obtained when analyzing the variation of n_k in terms of nonlinear trapping.

Of the experimental points of Fig. 5, however, only those corresponding to temperatures above 100 °K have real significance. Below 100 °K, compensational effects have to be taken into account when calculating the trapping factor. To illustrate this point, in Fig. 6 we have plotted theoretical curves for f_0 versus temperature with the parameter, $N_A/N_{D1} = 0$, 1, 4, and 8%, respectively, for the four curves. These curves were calculated from Eqs. (38) and (39) with $N_{D1} - N_A = 6.0 \times 10^{15}$ cm^{-3} and $E_{D1} = 52$ meV. Note that even the slightest degree of compensation drastically changes the form of f_0 at low temperatures. In the somewhat unrealistic approximation $N_A = 0$, f_0 saturates at a

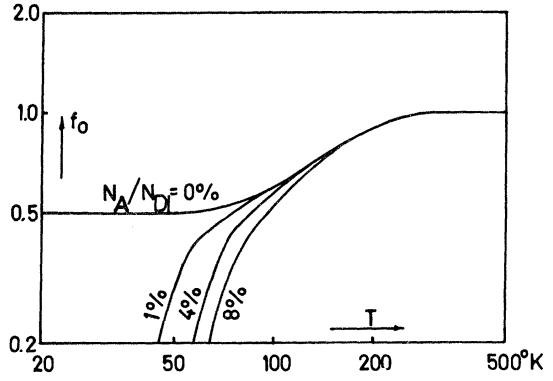

FIG. 6. Trapping factor f_0 as a function of temperature with the degree of compensation as a parameter, $N_A/N_{D1} = 0$, 1, 4, and 8%, respectively, for the four curves. The curves were calculated assuming a shallow-donor ionization energy of $E_{D1} = 52$ meV. Frequency-dependent trapping effects were neglected.

minimum value of 0.5 in the limit of very weak donor ionization. Adding a small number of acceptors, however, forces f_0 to approach zero when, at sufficiently low temperatures, $n_c \ll N_A$.

From Hall measurements on crystal No. 4A42, [24] the degree of compensation has been determined as $N_A/N_{D1} = 4\%$. As previously stated, compensational effects can then be expected at temperatures below 100 °K. Frequency-dependent trapping may set in at about the same temperature, giving us besides the degree of compensation yet another parameter to determine, i.e., the capture cross section S_n. Unfortunately, the experimental data do not permit us to determine N_A/N_{D1} and S_n separately. This is because the effect upon the variation of the apparent electron density of decreasing the capture cross section can be more or less compensated by assuming a larger acceptor density. Since N_A/N_{D1} has already been obtained from Hall experiments, we shall confine ourselves to determining S_n. In the following analysis, we therefore adopt the values $E_{D1} = 52$ meV and $N_A/N_{D1} = 4\%$ obtained by Galster[24] from his Hall measurements on crystal No. 4A42.

B. Capture Cross Section for Shallow Donors

With decreasing temperature, as more and more electrons freeze out, the rate of communication between conduction band and shallow donors rapidly decreases and eventually the trap relaxation time τ may become large enough for frequency-dependent trapping to set in. According to Eqs. (40), τ continues to increase until at a temperature T_A, $n_c = N_A$. For still lower temperatures, variations of n_c have little influence upon τ, the temperature dependence of which will now mainly be controlled by the factor $(v_{th}S_n)^{-1}$.

For crystal No. 4A42, $T_A = 68$ °K. Since T_A falls below 77 °K, the lowest temperature achieved during the present experiments, we expect the temperature dependence of τ to be mainly controlled by the free-electron density at all temperatures of interest. This implies that no detailed knowledge as to the temperature variation of $v_{th}S_n$ will be required for interpreting our experimental results. Hence, we shall not further discuss this problem but in connection with the determination of the absolute value of S_n at 100 °K assume a temperature variation for the capture cross section according to[30]

$$S_n = S_{n1}(100\,^\circ\mathrm{K}/T)^2. \tag{48}$$

A normalization temperature of 100 °K has been chosen because frequency-dependent trapping sets in at about this temperature. Thus, S_{n1} is the cross section that is directly obtainable from our measurements.

In Fig. 7, we have plotted the trap relaxation time as a function of temperature with the degree of compensation as a parameter, $N_A/N_{D1} = 0$, 4, and 8%, respectively, for the three curves. Since the average time an electron spends in the conduction band before being captured into a shallow-donor state depends inversely upon the density of ionized donors, the presence of acceptors which empty donor states tends to reduce the trap relaxation time. The curves were calculated from (38) and (40) with $E_{D1} = 52$ meV and $N_{D1} - N_A = 6.0 \times 10^{15}$ cm^{-3}. For the capture cross section at 100 °K, we have assumed $S_{n1} = 5 \times 10^{-12}$ cm^2 (see below). Consistent with the above discussion, τ increases drastically with decreasing temperature over the whole range of interest, i.e., above 77 °K. For any finite acceptor concentration, τ then goes through a maximum and approaches zero at low temperatures proportional to $(v_{th}S_n)^{-1}$ or, equivalently, proportional to $T^{3/2}$.

When the trap relaxation time becomes comparable to the dominant acoustic period, the phase shift of the free-electron modulation relative to the total electron density wave has to be taken into account. In this case, the threshold drift velocity v_{c2} for an opposing acoustoelectric current needs no longer exceed the threshold drift velocity v_{c1} for electronic gain. As pointed out in relation to

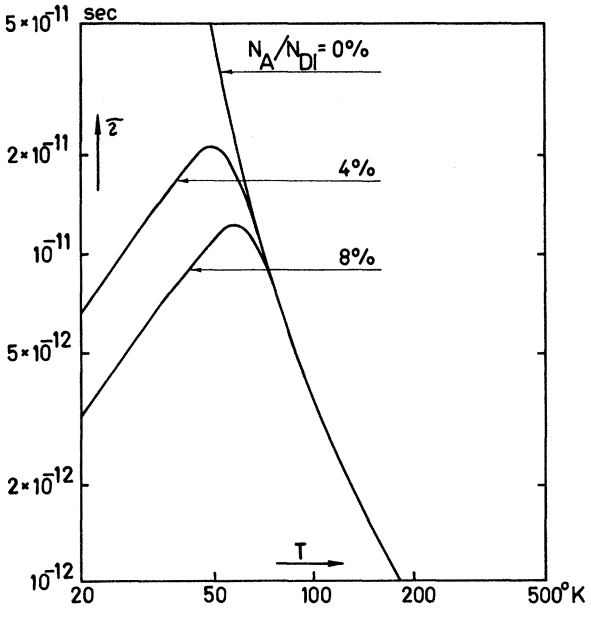

FIG. 7. Trap relaxation time τ as a function of temperature with the degree of compensation as a parameter, $N_A/N_{D1} = 0$, 4, and 8%, respectively, for the three curves. For the empty-donor capture cross section we have assumed a temperature variation according to $S_n = S_{n1}(100\,^\circ\mathrm{K}/T)^2$ with $S_{n1} = 5 \times 10^{-12}$ cm^2.

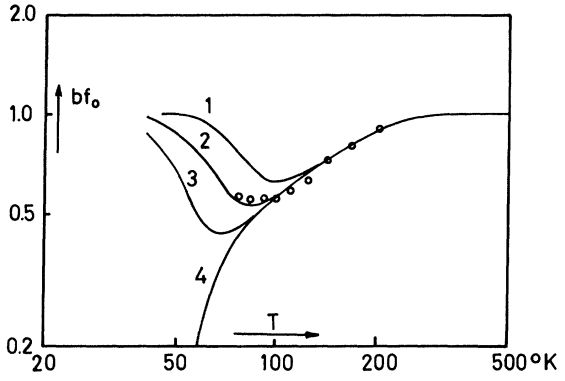

FIG. 8. bf_0 as a function of temperature for crystal No 4A42 (circles). Theoretical curves have been calculated assuming the values $S_{n1}=2\times10^{-12}\,\mathrm{cm}^2$(curve 1), $5\times10^{-12}\,\mathrm{cm}^2$ (curve 2), $10^{-11}\,\mathrm{cm}^2$ (curve 3), and $10^{-10}\,\mathrm{cm}^2$ (curve 4), respectively, for the capture cross section at 100 °K. The dominant acoustic frequency was taken to be $4\times10^{10}\,\mathrm{sec}^{-1}$.

our discussion of frequency-dependent trapping, however, the phase-shift correction tends to be particularly important when f_0 is very small, i.e., at low temperatures. Hence, we shall assume that a range of temperatures exists in which frequency-dependent trapping takes place and in which v_{c2} is still greater than v_{c1}. By analyzing the variation of n_k between 100 and 77 °K in terms of nonlinear frequency-dependent trapping, we obtain a value for S_{n1}. Using this value, we then calculate v_{c1} and v_{c2} and find that v_{c2} consistently will be greater than v_{c1} in the range of temperatures investigated. It turns out that only below 70 °K will v_{c1} be the greater.

In the general case, taking both frequency-dependent trapping and compensation into account, the critical electron densities n_{c1} and n_{c2} will be given by

$$n_{c1}=\frac{n_c v_{c1}}{v_s}=\frac{n_c[1+a(a+\omega/\omega_D)]}{bf_0} \tag{49}$$

and

$$n_{c2}=\frac{n_c v_{c2}}{v_s}=\frac{n_c}{[bf_0-\eta f_0(1-bf_0)]}\ . \tag{50}$$

Identifying now $n_k=n_{c2}$, Eq. (50) can be solved with respect to bf_0 to give

$$bf_0=\frac{n_c/n_k+\eta f_0}{1+\eta f_0}\ . \tag{51}$$

Here n_c and $\eta f_0=f_0 n_{D1}/N_{D1}$ are known quantities in the sense that they are independent of the capture cross section and can be calculated for specified values of N_{D1}, N_A, and E_{D1}.

In Fig. 8, we have plotted (circles) bf_0 as a function of temperature as calculated from (51) using our experimental values for n_k. Appropriate values for n_c and ηf_0 were computed using $E_{D1}=52$ meV, $N_{D1}-N_A=6.0\times10^{15}\,\mathrm{cm}^{-3}$, and $N_A/N_{D1}=4\%$. Also shown in this figure is a set of theoretical curves for bf_0 versus temperature corresponding to $S_{n1}/\omega=5\times10^{-23}\,\mathrm{cm}^2\,\mathrm{sec}$, $1.25\times10^{-22}\,\mathrm{cm}^2\,\mathrm{sec}$, $2.5\times10^{-22}\,\mathrm{cm}^2\,\mathrm{sec}$, and $2.5\times10^{-21}\,\mathrm{cm}^2\,\mathrm{sec}$, respectively, for the four curves. The curves were calculated from Eq. (17) with f_0 and as given by Eqs. (39) and (40). The above values for $N_{D1}-N_A$, N_A/N_{D1}, and E_{D1} were used.

The general shape of the theorectical curves is seen to reproduce the experimental values for bf_0 fairly well for a choice of S_{n1}/ω of about $1.25\times10^{-22}\,\mathrm{cm}^2\,\mathrm{sec}$. Consistent with our previous discussion (Sec. III), we may take $\omega=4\times10^{10}\,\mathrm{sec}^{-1}$ to be the dominant acoustic frequency at all temperatures. In this case, we obtain at 100 °K for the capture cross section $S_{n1}=5\times10^{-12}\,\mathrm{cm}^2$. Note, however, that the parameter determined when adjusting the theoretical curve for bf_0 to the experimental points is S_{n1}/ω rather than S_{n1}. Thus, the result for S_{n1} depends upon the acoustic frequency assumed to be dominant.

To the best of the author's knowledge, capture cross sections for shallow donors in ZnO have not previously been measured. Direct comparison with other materials is not possible because the capture cross section will depend not only on the geometrical extent of the attractive potential but also on the probability that an electron passing through this potential will give up sufficient energy in scattering processes to be captured. Measurements on Ge and Si [31] have yielded values between 10^{-15} and $10^{-12}\,\mathrm{cm}^2$ for the capture cross section of attractive impurity centers. In their analysis of trapping effects in semiconducting CdS, Moore and Smith[4] use a capture cross section of $1.4\times10^{-14}\,\mathrm{cm}^2$ at 50 °K to determine the dominant acoustic frequency of the internal generated acoustic flux. This cross section was adopted from Ge, and Moore and Smith arrived at a dominant frequency of about $3\times10^8\,\mathrm{sec}^{-1}$. If, however, one reverses their argument and assumes the dominant acoustic frequency to be about half the frequency of maximum electronic gain, one arrives at a capture cross section of about $10^{-12}\,\mathrm{cm}^2$ at 50 °K.

In Fig. 9, we have plotted the critical electron densities n_{c1} and n_{c2} as functions of temperature using the value $S_{n1}=5\times10^{-12}\,\mathrm{cm}^2$ for the capture cross section at 100 °K. E_{D1}, N_{D1}, and N_A were chosen as usual. Also shown in this figure is a theoretical curve for the variation of the free-electron density n_c and experimental points for n_k (circles). The temperature variation of n_{c2} is seen to reproduce the experimental points fairly well. Particularly,

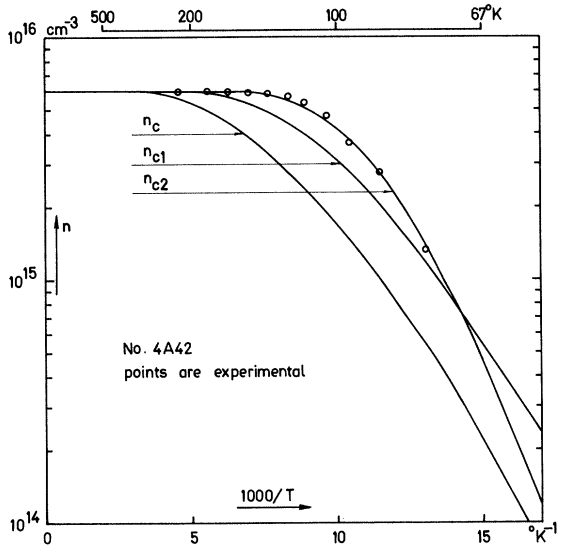

FIG. 9. Apparent electron density n_k (points) as a function of temperature for crystal No. 4A42. For comparison, we have plotted theoretical curves for the temperature variation of the free-electron density n_c and the critical electron densities

$$n_{c1}=\frac{n_c(1+a[a+\omega/\omega_D])}{bf_0}$$

and

$$n_{c2}=n_c/[bf_0-\eta f_0(1-bf_0)].$$

n_{c2} reproduces the rather sharp shoulder whereas linear trapping tends to give a smoother variation for n_{c1}. Note that below 70 °K, n_{c1} will be the greater and linear trapping will determine the threshold for current saturation.

C. Activation Energy for Deep Donors

So far, we have discussed the variation of the apparent electron density n_k at temperatures below 200 °K. At these temperatures, the apparent electron density is controlled by the distribution of electrons between conduction-band and shallow-donor states. At 200 °K, the plateau level of the n_k-versus-temperature curve is well established. According to our interpretation, this implies that $n_k = N_{D1} - N_A$, and, consequently, the shallow donors can cause no further increase of n_k. The growth of n_k at temperatures above 200 °K, therefore, requires for its explanation the assumption of an additional donor level.[6] In agreement with this conclusion, recent Hall experiments[24] have indicated the presence in our ZnO crystals of a deep-donor level.

To determine the activation energy for these deep donors, we have extended our measurements of saturated current-voltage characteristics towards higher temperatures and have reached a new plateau level for the apparent electron density at about 600 °K. This plateau corresponds, we assume, to $n_k = N_{D2} + N_{D1} - N_A$, where N_{D2} is the density of deep donors.

In general, the contribution to the apparent electron density due to the presence of deep donors may be expressed by ($T > 200$ °K)

$$n_{k2}(T) = n_k(T) - n_k(200\ ^\circ\mathrm{K}). \tag{52}$$

In Fig. 10, experimental values for n_{k2} have been plotted versus temperature for three different samples.

At temperatures above 600 °K, nearly all deep donors are ionized. With decreasing temperature, the deep donors start to capture free electrons, and trapping effects can be expected. As was the case for the shallow donors, the communication between free and bound states will be rapid at high temperatures where the electron freeze out has just begun. Hence, we can apply the frequency-independent trapping theory to analyze the variation of n_k at temperatures just below 600 °K. Note that because practically all shallow donors will be ionized at these high temperatures, this problem is also essentially a single-trap-level problem.

The condition of neutrality now reads

$$N_{D2} + N_{D1} = N_A + n_c + n_{D2}\,, \tag{53}$$

where n_{D2} is the density of electrons bound in deep-donor states. By means of Eq. (53), $n_D = n_{D2}$ can be eliminated from Eqs. (3) and (11) to give

$$\frac{n_c(n_c - N_{D1} + N_A)}{N_c(N_{D2} + N_{D1} - N_A - n_c)} = g^{-1}\, e^{-E_{D2}/kT} \tag{54}$$

and

$$f_0^{-1} = 1 + (N_{D2} + N_{D1} - N_A - n_c)(n_c - N_{D1} + N_A)/n_c N_{D2}\,. \tag{55}$$

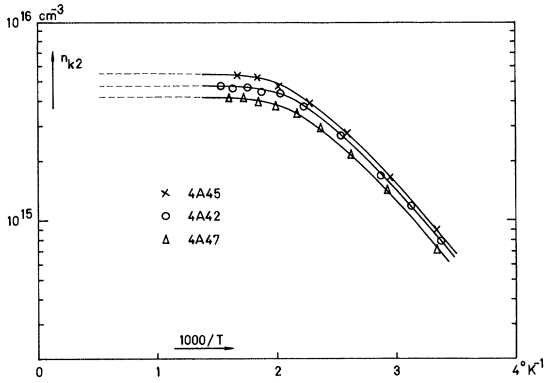

FIG. 10. n_{k2} as a function of temperature for three different samples. $n_{k2} = n_k(T) - n_k(200\ ^\circ\mathrm{K})$ is the contribution to the apparent electron density due to the presence of deep donors.

As more and more electrons are captured into deep-donor states, according to Eq. (55), f_0 starts to decrease from unity and reaches a minimum value of

$$f_{0m} = N_{D2}/\{N_{D2} + [(N_{D2} + N_{D1} - N_A)^{1/2} - (N_{D1} - N_A)^{1/2}]^2\} \tag{56}$$

for

$$n_c = [(N_{D2} + N_{D1} - N_A)(N_{D1} - N_A)]^{1/2} . \tag{57}$$

For still lower temperatures, f_0 then increases and approaches unity in the limit of very weak deep-donor ionization. A range of temperatures may then exist where practically all deep donors are occupied and at the same time all shallow donors are ionized. In this case, no bound electron density wave can be produced and trapping effects will be absent ($f_0 = 1$).

For crystal No. 4A42 using $N_{D2} + N_{D1} - N_A = 10.8 \times 10^{15}$ cm^{-3} and $N_{D1} - N_A = 6.0 \times 10^{15}$ cm^{-3} corresponding to the two plateau levels for the apparent electron density, we estimate the minimum trapping factor to be $f_{0m} = 0.87$. Thus, the trapping factor will be rather close to unity in the temperature range considered, i.e., between 200 and 640 °K, and consequently the deep-donor level gives rise to moderate trapping effects only. Further, the ratio v_{c2}/v_{c1} between our two critical drift velocities will be close to unity, which implies that it will be difficult to decide whether linear or nonlinear trapping control the threshold for current saturation in this temperature range. This is particularly so because we have no detailed information about nonelectronic acoustic losses at these high temperatures. Hence, we shall analyze the temperature variation of the apparent electron density in terms of the linear as well as the nonlinear trapping theory.

In the case of frequency-independent trapping ($bf_0 = f_0$, $a = 0$), the critical electron densities n_{c1} and n_{c2} will be given by

$$n_{c1} = n_c v_{c1}/v_s = n_c/f_0 \tag{58}$$

and

$$n_{c2} = n_c v_{c2}/v_s = n_c/[f_0 - \eta f_0(1 - f_0)] , \tag{59}$$

with

$$\eta = n_{D2}/N_{D2} = (N_{D2} + N_{D1} - N_A - n_c)/N_{D2} . \tag{60}$$

Assuming linear trapping effects to determine the threshold for current saturation, we replace n_{c1} by the apparent electron density n_k. The thermal equilibrium free-electron density n_c can then be eliminated from (55) and (58) to give a relation between f_0 and n_k with N_{D2} and $N_{D1} - N_A$ as parameters. By means of this relation, we have plotted in Fig. 11 (crosses) f_0 as a function of temperature for crystal No. 4A42. For N_{D2} and $N_{D1} - N_A$, we have used the values 4.8×10^{15} cm^{-3} and 6.0×10^{15} cm^{-3}, respectively. Assuming, on the other hand, nonlinear trapping to determine the threshold for current saturation, we replace n_{c2} by n_k and eliminate n_c from Eqs. (55), (59), and (60) to obtain a new relation between f_0 and n_k. This relation was then used to calculate another set of experimental points (circles in Fig. 11) for the variation of f_0 with temperature. Further, we have plotted in this figure (solid curve) two theoretical curves for the variation of f_0 with temperature corresponding to $E_{D2} = 200$ and 250 meV, respectively. These curves were calculated from Eqs. (54) and (55) using the above values for N_{D2} and $N_{D1} - N_A$. The donor degeneracy factor was taken to be $g = 2$. The dotted curve also plotted in Fig. 11 shows the variation of the trapping factor associated with electron density modulations on the shallow donors. In the temperature range between 200 and 350 °K, both shallow and deep donors apparently give rise to trapping effects. For at least one of the two types of donor centers, however, the trapping effects will always be negligible and hence we shall not discuss the double-trap-level problem. We may recall, however, that Hutson and White[7] have analyzed linear frequency-independent trapping for the general case of several kinds of trapping center.

The theoretical curves are seen to reproduce the experimental points fairly well for a choice of the deep-donor activation energy between 220 and 240 meV. Since we do not know whether linear or non-

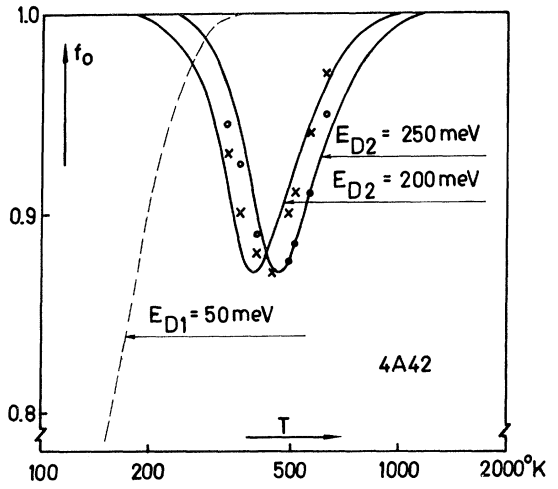

FIG. 11. Trapping factor f_0 as a function of temperature for crystal No. 4A42. The two theoretical curves were calculated for a deep-donor ionization energy of 200 and 250 meV, respectively. The two sets of experimental points were obtained by analyzing the temperature variation of the apparent electron density n_k in terms of linear (crosses) and nonlinear (circles) trapping effects, respectively. The dotted curve shows the trapping factor associated with the shallow-donor traps.

linear trapping effects will dominate, we shall attribute the same weight to our two sets of experimental results (crosses and circles in Fig. 11). We may then estimate the activation energy to be $E_{D2} = 230$ meV. For comparison, Hall measurements[24] on crystal No. 4A42 have given a deep-donor ionization energy of about 200 meV.

From the general agreement between experiments and frequency-independent trapping theory, we are led to assume that the communication between conduction-band and deep-donor states is sufficient for frequency-dependent trapping effects to be negligible above 350 °K. This implies that $\omega\tau < 0.3$ at these temperatures, and, consequently, assuming the dominant acoustic frequency to be $\omega = 4\times10^{10}$ sec^{-1}, the deep-donor capture cross section $S_{n2} > 10^{-13}$ cm^2 at 350 °K.

V. DISCUSSION

So far, we have concerned ourselves entirely with the knee point of the current-voltage characteristics. This is a region where the linear theory of acoustoelectric coupling presumably can be used to evaluate the quantities γ and δn_c entering our expression (29) for the acoustoelectric current.

At temperatures below 94 °K, the I-V curves of Fig. 1 reveal another interesting feature besides the current saturation. Above a certain average field F_j, the current jumps through saturation into a region where different modes of current oscillations are found. A similar behavior of the I-V curves was observed by Moore and Smith[4] for semiconducting CdS below 60 °K. By means of pulsed Hall measurements, Moore and Smith showed that the average electron drift velocity was saturated close to the velocity of sound over the entire range of current oscillations and thus concluded that the break in saturation was due to an increased free-electron density. They proposed impact ionization of the donor traps by hot electrons as a possible mechanism. Since the average electron energy at F_j is still close to thermal energy, the electronic breakdown must be ascribed to those few carriers which may escape the sound barrier. For this explanation, the presence of a stationary high-field region at the downstream end of the saturated crystal is an important assumption because such a high-field region is required for the few carriers escaping the sound barrier to heat up.

A strong anode field is usually found in acoustoelectrically saturated samples[3] and is found as well in our ZnO crystals at room temperature.[32] Probe measurements on saturated ZnO single crystals at 77 °K,[6] however, have shown that any particularly strong anode field does not build up at this temperature. The field distribution along ZnO crystals at 77 °K was investigated by placing six point probes along the surface. The probes were spaced 0.6 mm from each other with probe No. 1 situated close to the cathode end and probe No. 6 close to the anode end of the crystal. When the average field F was increased above the knee-point field F_k, the slope of the voltage V_{45} (between probe Nos. 4 and 5) as a function of F first increased by a factor of about 2 and then gradually decreased towards 0 with V_{45} saturating at a voltage corresponding to an average field strength between the probes of about 2.5 kV/cm. With increasing F, as V_{45} starts to saturate, the same kind of change was observed for the slope of the voltage V_{34} so that the high-field region was extending over an increasing part of the crystal. With further increase of F, the high-field region continued to grow towards the cathode until at the jump field F_j the field distribution along the crystal was almost uniform, with the field nowhere exceeding 3 kV/cm.

At such low fields, impact ionization of donor atoms with an activation energy of about 50 meV seems unlikely. We may therefore suggest that the nonlinear trapping mechanism is responsible for the break in saturation, i.e., that the ionization of the shallow-donor states is caused by the intense acoustic flux rather than by hot electrons.

In the strongly nonlinear region above F_k, the trapping theory presented in this work has no quantitative validity since we have everywhere used the small signal approximation[7] to express the total electron density wave n_s in terms of the acoustic strain amplitude. In particular, the theory only holds as long as $\delta n_c \lesssim n_D$, since otherwise, according to Eq. (26), the average density of bound electrons would be negative. We may emphasize, however, that in the case of frequency-independent trapping, our simple theory [Eq. (44)] predicts infinite values for the critical electron density n_{c2} when the trapping factor reaches values as small as $f_0 = \frac{1}{2}[3-(5)^{1/2}] = 0.38$. We may suggest that the pole for n_{c2} in the simple theory corresponds to the complete ionization of the shallow donors in a more elaborate theory.

It is well established by now[23,33] that the dominant acoustic frequency in the current-saturated region falls below the linear frequency of maximum net gain. The downshift of the frequency of maximum intensity may be caused by parametric amplification[34] or by carrier bunching effects.[35]

In the case of frequency-dependent trapping, the critical electron density n_{c2} depends upon the acoustic frequency through the function bf_0. This relation is such that n_{c2} increases for decreasing acoustic frequency. Thus, as the dominant acoustic frequency decreases by virtue of the above mentioned nonlinear mechanisms, n_{c2} increases and eventually the current may break through saturation when the

high-flux region extends over the entire crystal.

ACKNOWLEDGMENTS

The author wishes to thank Professor N. I. Meyer for his encouragement and for many valuable suggestions. Dr. M. H. Joergensen is acknowledged for a number of very stimulating discussions on trapping theory, as well as for advice about the experiments. The author is indebted to Dr. G. Galster for making his Hall data available prior to publication and to Dr. C. Hurwitz for helpful comments on the manuscript.

[1]A. R. Hutson, Phys. Rev. 108, 222 (1957).

[2]R. W. Smith, Phys. Rev. Letters 9, 87 (1962).

[3]J. H. McFee, J. Appl. Phys. 34, 1548 (1963).

[4]A. R. Moore and R. W. Smith, Phys. Rev. 138, A1250 (1965).

[5]A. Rannestad, Phys. Rev. 155, 744 (1967).

[6]N. I. Meyer, M. H. Joergensen, and E. Mosekilde, J. Phys. Soc. Japan Suppl. 21, 406 (1966).

[7]A. R. Hutson and D. L. White, J. Appl. Phys. 33, 40 (1962).

[8]D. L. White, J. Appl. Phys. 33, 2547 (1962).

[9]A. R. Hutson, Phys. Rev. Letters 9, 296 (1962).

[10]G. Weinreich, Phys. Rev. 104, 321 (1956).

[11]I. Uchida, T. Ishiguro, Y. Sasaki, and T. Suzuki, J. Phys. Soc. Japan 19, 674 (1964).

[12]C. A. A. J. Greebe, Phys. Letters 4, 45 (1963).

[13]C. A. A. J. Greebe, Philips Res. Rept. 21, 1 (1966).

[14]P. D. Southgate and H. M. Spector, J. Appl. Phys. 36, 3728 (1965).

[15]R. Kailyus, Fiz. Tverd. Tela 10, 458 (1968) [Soviet Phys. Solid State 10, 359 (1968)].

[16]Shining light onto a photoconducting medium, among all excited electrons $n+n_t$ some electrons n will be free to drift in an applied field and to recombine. Others n_t, however, may be trapped in bound states from which recombination is unlikely. These latter electrons will then have to be thermally reexcited into the conduction band before recombination can take place. To account for this situation, the theory of photoconductivity [see, e.g., R. Bube, *Photoconductivity* (Wiley, New York, 1960), p. 68] defines a large signal trapping factor $f_t = n/(n+n_t)$. By definition, f_t differs from the small signal trapping factor f_0 defined in Ref. 7. For strongly compensated materials, however, f_0 takes the form $f_0 = n_c/(n_c+n_D)$ which is formally equivalent to the above expression for f_t.

[17]R. H. Parmenter, Phys. Rev. 89, 990 (1953).

[18]N. I. Meyer and E. Mosekilde, Phys. Letters 24, A115 (1967).

[19]Yu. V. Gulyaev, Fiz. Tekh. Poluprovodnikov 2, 628 (1968) [Soviet Phys. Semicond. 2, 525 (1968)].

[20]A somewhat similar situation arises when considering acoustodynamic effects in intrinsic semiconductors which contain holes as well as electrons. As pointed out by Weinreich (Ref. 10) one will have to consider carrier recombination to the second order in the wave amplitudes to correctly calculate the acoustelectric current in this case.

[21]K. F. Nielsen, J. Crystal Growth 3, 141 (1968).

[22]J. H. McFee, J. Appl. Phys. 34, 1548 (1963).

[23]W. Wettling and M. Bruun, Phys. Letters 27, A123 (1968).

[24]G. Galster (unpublished).

[25]B. K. Ridley and J. Wilkinson, J. Phys. C 2, 1299 (1969).

[26]R. B. Hemphill, Appl. Phys. Letters 9, 35 (1966).

[27]D. F. Crisler, J. J. Cupal, and A. R. Moore, Proc IEEE 56, 225 (1968).

[28]When considering the temperature variation of the critical electron density n_{c1}, we may neglect the difference between the threshold drift velocity for electronic amplification and the threshold for net acoustic gain, the difference being a few percent at all temperatures of interest.

[29]A. R. Hutson, J. Appl. Phys. 32, 2287 (1961); see also Ref. 23.

[30]See Ref. 4 and references cited therein.

[31]M. Lax, J. Phys. Chem. Solids 8, 66 (1959).

[32]M. Bruun, M. H. Joergensen, N. I. Meyer, and E. Mosekilde, in Proceedings of the International Conference on Semiconductor Physics, Moscow, 1968 (unpublished).

[33]J. Zucker, S. Zemon , and J. H. Wasko, in *Proceedings of the International Conference on II–VI Semiconducting Components, Providence, Rhode Island*, 1967 (Benjamin, New York, 1968).

[34]S. Zemon, J. Zucker, J. H. Wasko, E. M. Conwell, and A. K. Ganguly, Appl. Phys. Letters 12, 378 (1968).

[35]P. N. Butcher and N. Ogg, Brit. J. Appl. Phys. D 1, 1271 (1968).